

Robust Fixed-Interval Smoothing for the Estimation of Optical Phase Varying as a Continuous Resonant Process[#]

Shibdas Roy^{1*}, Obaid Ur Rehman², Ian R. Petersen³ and Elanor H. Huntington⁴

Abstract—Precise tracking of a randomly varying optical phase is key to metrology, with applications in optical communication. Continuous phase estimation is known to be superior in accuracy as compared to static estimation. The underlying parameters in the signal model or the measurement itself are, however, prone to changes owing to unavoidable external noises or apparatus imperfections. The estimation process is, thus, desired to be made robust to uncertainties in these parameters. Here, homodyne phase estimations of coherent and squeezed states of light, evolving continuously under the influence of a resonant noise process, are made robust to parameter uncertainties using a robust fixed-interval smoother, designed for uncertain systems satisfying a certain integral quadratic constraint.

I. INTRODUCTION

The quantum phase estimation [1] is central to various fields such as metrology [2], quantum computation [3], communication [4], [5] and quantum cryptography [6]. A fundamental bound on the estimation accuracy is imposed by Heisenberg's uncertainty principle [7], that, for example, limits gravitational wave detection [8]. A less fundamental yet practically relevant limit, called the standard quantum limit (SQL), is the minimum level of quantum noise obtained using standard approaches without real-time feedback. The SQL sets an important benchmark for the quality of an estimation process and calls for devising quantum strategies that can beat it.

Real-time feedback in homodyne estimation of a *static* unknown phase can yield mean-square errors lower than the SQL [9], [10], [11], [12] or even reaching the theoretical limit [13]. However, it is experimentally more relevant to precisely estimate a phase, that is *continuously varying* under the influence of an unmeasured classical noise process [14], [15], [16], [17]. A classical process coupled dynamically to a quantum system under continuous measurement may be estimated in various ways: prediction, filtering or smoothing [18]. In particular, smoothing uses both past and future measurements to yield a more accurate estimate than filtering alone, that uses only past measurements. Since smoothing is non-causal, it cannot be used in real-time, but is used for offline data processing or with a delay with respect to the estimation time.

The *fixed-interval* smoothing problem [19], [20], [21] considers measurements over a fixed time-interval T , where

the estimation time is $t < T$. One solution, the Mayne-Fraser two-filter smoother [22], [23], [24], consists of a forward-time Kalman filter and also a backward-time Kalman filter called an “information filter” [25] and it combines the two estimates to yield the optimal smoothed estimate. The information filter and the smoother were combined into a single backward smoother by Rauch, Tung and Striebel (RTS) [26], [27].

In Refs. [16], [17] the signal phase to be estimated is allowed to evolve under the influence of an unmeasured continuous-time Ornstein-Uhlenbeck (OU) noise process. However, the estimation process heavily relies on the underlying parameters being precisely known, which is practically not feasible due to unavoidable external noises and/or apparatus imperfections. It is, therefore, desired to make the estimation process robust to uncertainties in these parameters to improve the quality of the phase measurement. In Ref. [28] the authors have shown that a robust guaranteed cost filter [29] yields better accuracy in the phase estimate than an optimal Kalman filter with parameter uncertainty in the phase being measured. The authors have also demonstrated improvement in continuous phase estimation with robust fixed-interval smoothing [30] as compared to optimal RTS smoothing for a coherent state [31] and a squeezed state [32] of light.

These works, however, considered a simplistic Ornstein-Uhlenbeck noise process modulating the signal phase to be estimated, and the kind of noises that in practice corrupt the signal are more complicated than an OU process. The authors have illustrated in Ref. [33] a guaranteed cost robust filter designed for a more complicated and practically relevant second-order resonant noise process. Here, we design a robust fixed-interval smoother [30], meant for uncertain systems admitting a certain integral quadratic constraint, for coherent light beam phase-modulated by such a resonant noise process. We compare the performance of the robust and RTS smoothers for the uncertain system with respect to the standard quantum limit. We also extend this by designing such a robust fixed-interval smoother for a phase-squeezed light beam and compare its behaviour with a corresponding RTS smoother in relation to the coherent state limit (CSL). The coherent state limit determines the minimum estimation error that can be obtained for a coherent state of light.

II. RESONANT NOISE PROCESS

The resonant noise process under consideration in this paper is typically generated by a piezo-electric transducer (PZT) driven by an input white noise. The simplified transfer

[#]This work was supported by the Australian Research Council.

¹S. Roy, ²O. Rehman, ³I. R. Petersen and ⁴E. H. Huntington are with the School of Engineering and Information Technology, University of New South Wales, Canberra.

*shibdas.roy at student.adfa.edu.au

function of a typical PZT is given by:

$$G(s) := \frac{\phi}{v} = \frac{\kappa}{s^2 + 2\zeta\omega_r s + \omega_r^2}, \quad (1)$$

where κ is the gain, ζ is the damping factor, ω_r is the resonant frequency (rad/s) and v is a zero-mean white Gaussian noise with unity amplitude.

We use the following values for the parameters above: $\kappa = 9 \times 10^4$, $\zeta = 0.01$ and $\omega_r = 6.283 \times 10^3$ rad/s (1 kHz). Fig. 1 shows the Bode plot of the transfer function (1).

Let $x_1 := \phi$ and $x_2 := \dot{\phi}$. A state-space realization of the transfer function (1) is:

$$\dot{\mathbf{x}} = \mathbf{A}\mathbf{x} + \mathbf{G}v, \quad (2)$$

where

$$\mathbf{x} := \begin{bmatrix} x_1 \\ x_2 \end{bmatrix}, \quad \mathbf{A} := \begin{bmatrix} 0 & 1 \\ -\omega_r^2 & -2\zeta\omega_r \end{bmatrix}, \quad \mathbf{G} := \begin{bmatrix} 0 \\ \kappa \end{bmatrix}.$$

III. COHERENT STATE: OPTIMAL SMOOTHER

The homodyne “smoothed” phase estimation of a weak coherent state of light is optimal for given values of the parameters when using an offline RTS estimator alongwith a Kalman filter in the feedback loop to adjust the phase of the local oscillator. Under a linearization approximation, the homodyne photocurrent from the phase estimation system is given by [16]:

$$I(t)dt = 2|\alpha|[\phi(t) - \hat{\phi}(t)]dt + dW(t), \quad (3)$$

where $|\alpha|$ is the amplitude of the coherent state with photon flux given by $\mathcal{N} := |\alpha|^2$, $\hat{\phi}$ is the *intermediate phase estimate*, and $W(t)$ is a Wiener process arising from the quantum vacuum fluctuations.

The measurement model is, thus, [33]:

$$\theta = \mathbf{H}\mathbf{x} + \mathbf{J}w, \quad (4)$$

where $w := \frac{dW}{dt}$ is a zero-mean Gaussian white noise with unity amplitude and $\mathbf{H} := \begin{bmatrix} 2|\alpha| & 0 \end{bmatrix}$ and $\mathbf{J} := 1$.

Rewriting the equations for the system under consideration, we get:

$$\begin{aligned} \text{Process model: } \dot{\mathbf{x}} &= \mathbf{A}\mathbf{x} + \mathbf{G}v, \\ \text{Measurement model: } \theta &= \mathbf{H}\mathbf{x} + \mathbf{J}w, \end{aligned} \quad (5)$$

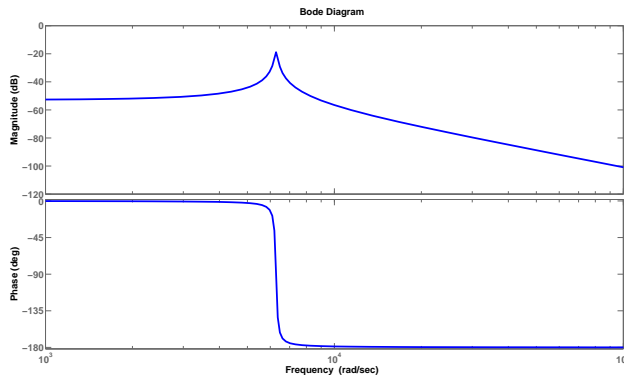


Fig. 1. Bode plot of the resonant noise process transfer function.

where

$$\begin{aligned} E[v(t)v(\tau)] &= \mathbf{N}\delta(t - \tau), \\ E[w(t)w(\tau)] &= \mathbf{S}\delta(t - \tau), \\ E[v(t)w(\tau)] &= 0. \end{aligned}$$

Since v and w are unity amplitude white noise processes, both \mathbf{N} and \mathbf{S} are unity (scalars).

A. Forward Kalman Filter

The continuous-time algebraic Riccati equation to be solved to construct the steady-state forward Kalman filter is [34]:

$$\mathbf{A}\mathbf{P}_f + \mathbf{P}_f\mathbf{A}^T + \mathbf{G}\mathbf{N}\mathbf{G}^T - \mathbf{P}_f\mathbf{H}^T(\mathbf{J}\mathbf{S}\mathbf{J}^T)^{-1}\mathbf{H}\mathbf{P}_f = \mathbf{0}. \quad (6)$$

The forward Kalman filter equation is [34]:

$$\dot{\hat{\mathbf{x}}} = (\mathbf{A} - \mathbf{K}_f\mathbf{H})\hat{\mathbf{x}} + \mathbf{K}_f\mathbf{H}\mathbf{x} + \mathbf{K}_f\mathbf{J}w, \quad (7)$$

where $\mathbf{K}_f := \mathbf{P}_f\mathbf{H}^T(\mathbf{J}\mathbf{S}\mathbf{J}^T)^{-1}$ is the Kalman gain.

B. Backward Kalman Filter

The continuous-time algebraic Riccati equation to be solved to construct the steady-state backward Kalman filter is [27]:

$$-\mathbf{A}\mathbf{P}_b - \mathbf{P}_b\mathbf{A}^T + \mathbf{G}\mathbf{N}\mathbf{G}^T - \mathbf{P}_b\mathbf{H}^T(\mathbf{J}\mathbf{S}\mathbf{J}^T)^{-1}\mathbf{H}\mathbf{P}_b = \mathbf{0}. \quad (8)$$

The backward Kalman filter equation is [27]:

$$\dot{\hat{\mathbf{x}}} = (-\mathbf{A} - \mathbf{K}_b\mathbf{H})\hat{\mathbf{x}} + \mathbf{K}_b\mathbf{H}\mathbf{x} + \mathbf{K}_b\mathbf{J}w, \quad (9)$$

where $\mathbf{K}_b := \mathbf{P}_b\mathbf{H}^T(\mathbf{J}\mathbf{S}\mathbf{J}^T)^{-1}$ is the Kalman gain.

C. Smoother Error

The smoother error covariance matrix is obtained as:

$$\mathbf{P}_s = (\mathbf{P}_f^{-1} + \mathbf{P}_b^{-1})^{-1}, \quad (10)$$

since the forward and backward estimates of the optimal (Kalman) smoother are independent [27].

Using $\kappa = 9 \times 10^4$, $\zeta = 0.01$ and $\omega_r = 6.283 \times 10^3$ rad/s (1 kHz) as in section II and $|\alpha| = 5 \times 10^2$, we get:

$$\mathbf{P}_s = \begin{bmatrix} 3.7998657 \times 10^3 & 0 \\ 0 & 3.7344282 \times 10^5 \end{bmatrix}. \quad (11)$$

IV. COHERENT STATE: ROBUST SMOOTHER

In this section, we make our smoother robust to uncertainties in the parameters underlying the system matrix \mathbf{A} using the robust fixed-interval smoothing approach from Ref. [30].

We introduce uncertainty in \mathbf{A} as follows:

$$\mathbf{A} \rightarrow \mathbf{A} + \begin{bmatrix} 0 & 0 \\ -\mu_1\delta_1\omega_r^2 & -2\mu_2\delta_2\zeta\omega_r \end{bmatrix},$$

where $\Delta := \begin{bmatrix} \delta_1 & \delta_2 \end{bmatrix}$ is an uncertain parameter satisfying $\|\Delta\| \leq 1$ that implies $\delta_1^2 + \delta_2^2 \leq 1$. $0 \leq \mu_1 < 1$, $0 \leq \mu_2 < 1$ are parameters determining the levels of uncertainty.

Thus, the process and measurement models of (5) take the form:

$$\begin{aligned} \text{Process model: } \dot{\mathbf{x}} &= (\mathbf{A} + \mathbf{G}\Delta\mathbf{K})\mathbf{x} + \mathbf{G}v, \\ \text{Measurement model: } \theta &= \mathbf{H}\mathbf{x} + \mathbf{J}w, \end{aligned} \quad (12)$$

where $\mathbf{K} := \begin{bmatrix} -\frac{\mu_1 \omega_r^2}{\kappa} & 0 \\ 0 & -\frac{2\mu_2 \zeta \omega_r}{\kappa} \end{bmatrix}$.

The Integral Quadratic Constraint of Eq. (2.4) in Ref. [30] for our case is:

$$\int_0^T (\tilde{w}^2 + \tilde{v}^2) dt \leq 1 + \int_0^T \|\mathbf{z}\|^2 dt, \quad (13)$$

where $\mathbf{z} = \mathbf{K}\mathbf{x}$ is the *uncertainty output*, and $\tilde{w} = \Delta\mathbf{K}\mathbf{x} + v$ and $\tilde{v} = w$ are the *uncertainty inputs*. Thus, we would have $\mathbf{Q} = 1$ and $\mathbf{R} = 1$ in our case.

The steady-state forward Riccati equation, as obtained from Eq. (5.1) in Ref. [30] for our case, is:

$$\mathbf{Y}\mathbf{A} + \mathbf{A}^T\mathbf{Y} + \mathbf{Y}\mathbf{G}\mathbf{Q}^{-1}\mathbf{G}^T\mathbf{Y} + \mathbf{K}^T\mathbf{K} - \mathbf{H}^T\mathbf{R}\mathbf{H} = \mathbf{0}. \quad (14)$$

The steady-state backward Riccati equation, as obtained from Eq. (5.2) in Ref. [30] for our case, is:

$$\mathbf{Z}\mathbf{A} + \mathbf{A}^T\mathbf{Z} - \mathbf{Z}\mathbf{G}\mathbf{Q}^{-1}\mathbf{G}^T\mathbf{Z} - \mathbf{K}^T\mathbf{K} + \mathbf{H}^T\mathbf{R}\mathbf{H} = \mathbf{0}. \quad (15)$$

Next, Eq. (5.3) in Ref. [30] yields:

$$\dot{\eta} = -(\mathbf{A} + \mathbf{G}\mathbf{Q}^{-1}\mathbf{G}^T\mathbf{Y})^T\eta + \mathbf{H}^T\mathbf{R}\theta. \quad (16)$$

Likewise, Eq. (5.4) in Ref. [30] for reverse-time yields:

$$\dot{\xi} = (\mathbf{A} - \mathbf{G}\mathbf{Q}^{-1}\mathbf{G}^T\mathbf{Z})^T\xi + \mathbf{H}^T\mathbf{R}\theta. \quad (17)$$

The forward filter is simply the centre of the ellipse of Eq. (3.3) in Ref. [30]: $\hat{\mathbf{x}}_f = \mathbf{Y}^{-1}\eta$. Likewise, the backward filter is: $\hat{\mathbf{x}}_b = \mathbf{Z}^{-1}\xi$.

The robust smoother for the uncertain system would, then, be the centre of the ellipse of Eq. (5.5) in Ref. [30]:

$$\hat{\mathbf{x}} = (\mathbf{Y} + \mathbf{Z})^{-1}(\eta - \xi). \quad (18)$$

V. COHERENT STATE: COMPARISON FOR THE ROBUST AND KALMAN SMOOTHERS

A. Lyapunov Method

1) *Forward Filter*: We augment the system given by (12) with the forward Kalman filter (7) and represent the augmented system by the state-space model:

$$\dot{\bar{\mathbf{x}}} = \bar{\mathbf{A}}\bar{\mathbf{x}} + \bar{\mathbf{B}}\bar{\mathbf{w}}, \quad (19)$$

where

$$\bar{\mathbf{x}} := \begin{bmatrix} \mathbf{x} \\ \hat{\mathbf{x}} \end{bmatrix} \quad \text{and} \quad \bar{\mathbf{w}} := \begin{bmatrix} v \\ w \end{bmatrix}.$$

Thus, we have:

$$\bar{\mathbf{A}} = \begin{bmatrix} \mathbf{A} + \mathbf{G}\Delta\mathbf{K} & \mathbf{0} \\ \mathbf{K}_f\mathbf{H} & \mathbf{A} - \mathbf{K}_f\mathbf{H} \end{bmatrix}, \bar{\mathbf{B}} = \begin{bmatrix} \mathbf{G} & \mathbf{0} \\ \mathbf{0} & \mathbf{K}_f\mathbf{J} \end{bmatrix}.$$

For the continuous-time state-space model (19), the steady-state state covariance matrix \mathbf{P}_{fs} is obtained by solving the *Lyapunov equation*:

$$\bar{\mathbf{A}}\mathbf{P}_{fs} + \mathbf{P}_{fs}\bar{\mathbf{A}}^T + \bar{\mathbf{B}}\bar{\mathbf{B}}^T = \mathbf{0}, \quad (20)$$

where \mathbf{P}_{fs} is the symmetric matrix

$$\mathbf{P}_{fs} := E(\bar{\mathbf{x}}\bar{\mathbf{x}}^T) := \begin{bmatrix} \Sigma & \mathbf{M}_f \\ \mathbf{M}_f^T & \mathbf{N}_f \end{bmatrix}.$$

The state estimation error can be written as:

$$\mathbf{e}_f := \mathbf{x} - \hat{\mathbf{x}} = [\mathbf{1} \ -\mathbf{1}]\bar{\mathbf{x}},$$

which is mean zero since all of the quantities determining \mathbf{e}_f are mean zero.

The error covariance matrix is then given as:

$$\begin{aligned} \mathbf{\Pi}_f &:= E(\mathbf{e}_f\mathbf{e}_f^T) = [\mathbf{1} \ -\mathbf{1}]E(\bar{\mathbf{x}}\bar{\mathbf{x}}^T) \begin{bmatrix} \mathbf{1} \\ -\mathbf{1} \end{bmatrix} \\ &= [\mathbf{1} \ -\mathbf{1}] \begin{bmatrix} \Sigma & \mathbf{M}_f \\ \mathbf{M}_f^T & \mathbf{N}_f \end{bmatrix} \begin{bmatrix} \mathbf{1} \\ -\mathbf{1} \end{bmatrix} \\ &= \Sigma - \mathbf{M}_f - \mathbf{M}_f^T + \mathbf{N}_f. \end{aligned} \quad (21)$$

2) *Backward Filter*: The augmented system state-space model (19) for the backward Kalman filter (9) would have:

$$\bar{\mathbf{A}} = \begin{bmatrix} \mathbf{A} + \mathbf{G}\Delta\mathbf{K} & \mathbf{0} \\ \mathbf{K}_b\mathbf{H} & -\mathbf{A} - \mathbf{K}_b\mathbf{H} \end{bmatrix}, \bar{\mathbf{B}} = \begin{bmatrix} \mathbf{G} & \mathbf{0} \\ \mathbf{0} & \mathbf{K}_b\mathbf{J} \end{bmatrix}.$$

We then solve the *Lyapunov equation* (20), with \mathbf{P}_{fs} replaced by

$$\mathbf{P}_{bs} := E(\bar{\mathbf{x}}\bar{\mathbf{x}}^T) := \begin{bmatrix} \Sigma & \mathbf{M}_b \\ \mathbf{M}_b^T & \mathbf{N}_b \end{bmatrix},$$

for the backward filter.

The error covariance matrix is, thus:

$$\mathbf{\Pi}_b := E(\mathbf{e}_b\mathbf{e}_b^T) = \Sigma - \mathbf{M}_b - \mathbf{M}_b^T + \mathbf{N}_b. \quad (22)$$

3) *Cross-Correlation Term*: The forward and backward estimates are not independent and are correlated in this case, unlike in section III. The cross-correlation term is [31]:

$$\mathbf{\Pi}_{fb} := E(\mathbf{e}_f\mathbf{e}_b^T) = \Sigma - \mathbf{M}_f^T - \mathbf{M}_b + \alpha\Sigma\beta, \quad (23)$$

where $\alpha := \mathbf{M}_f^T\Sigma^{-1}$ and $\beta := \Sigma^{-1}\mathbf{M}_b$ [21].

4) *Smoother Error*: The smoother error covariance is [31]:

$$\mathbf{\Pi} := \frac{\mathbf{\Pi}_f\mathbf{\Pi}_b - \mathbf{\Pi}_{fb}^2}{\mathbf{\Pi}_f + \mathbf{\Pi}_b - 2\mathbf{\Pi}_{fb}}. \quad (24)$$

Since we are mainly interested in estimating $x_1 = \phi$, the estimation error covariance of interest is $\sigma^2 = \mathbf{\Pi}(1, 1)$.

B. Standard Quantum Limit

The standard quantum limit is set by the minimum phase estimation error that can be obtained using perfect heterodyne scheme. The heterodyne scheme of measurement incurs the same noise penalty as *dual-homodyne* scheme [16]. A schematic for the dual-homodyne scheme is depicted in Fig. 2. An electro-optic modulator (EOM), driven by the resonant noise source, phase-modulates the input signal. The modulated signal then splits through a 50 – 50 beamsplitter into two arms each with a homodyne detector (HD1 and HD2, respectively, with the local oscillator phase of HD1 $\pi/2$ out of phase with that of HD2). The *arctan* of the ratio of the output signals of the two arms is then fed into a low-pass filter (LPF). The phase estimation error would then be minimum if this LPF is an optimal Kalman filter.

The output signals of the two arms are:

$$I_1 = \frac{1}{\sqrt{2}} (2|\alpha| \sin \phi + n_1 + n_2),$$

$$I_2 = \frac{1}{\sqrt{2}} (2|\alpha| \cos \phi + n_3 - n_4),$$

where n_2 and n_4 are the noises arising from the vacuum entering the empty port of the input beamsplitter corresponding to the two arms, respectively, and n_1 and n_3 are measurement noises of the two homodyne detectors, respectively. All these noises are assumed to be zero-mean white Gaussian.

The output of the arctan block is:

$$\vartheta = \arctan \left(\frac{2|\alpha| \sin \phi + n_1 + n_2}{2|\alpha| \cos \phi + n_3 - n_4} \right). \quad (25)$$

Assuming the input noises are small, a Taylor series expansion upto first-order terms of the right-hand side yields:

$$\vartheta \approx \phi + \frac{1}{2|\alpha|} n_1 + \frac{1}{2|\alpha|} n_2. \quad (26)$$

Expressing this equation in terms of \mathbf{x} , we get the measurement model as:

$$\vartheta = \mathbf{H}\mathbf{x} + \mathbf{J}w, \quad (27)$$

where $\mathbf{H} = \begin{bmatrix} 1 & 0 \end{bmatrix}$ and $\mathbf{J} = \begin{bmatrix} \frac{1}{2|\alpha|} & \frac{1}{2|\alpha|} \end{bmatrix}$.

The error covariance matrix of the optimal steady-state Kalman filter for the process given by (2) and the measurement given by (27) is obtained by solving an algebraic Riccati equation of the form (6) for \mathbf{P}_f . The error covariance of interest (i.e. that in estimating $x_1 = \phi$) is then $\sigma^2 = \mathbf{P}_f(1, 1)$.

C. Comparison of Estimation Errors

The estimation mean-square errors may be calculated, as described in section V-A, for the Kalman smoother, and likewise for the robust smoother, as a function of the uncertain parameter δ_1 with $\delta_2 = 0$. Here, we use the nominal values of the parameters and choose different values for μ_1 and set $\mu_2 = 0$. These values were used to generate plots of the errors versus δ_1 to compare the performance of the robust smoother and the Kalman smoother for the uncertain system in comparison to the SQL. The SQL value is obtained by designing, as described in section V-B, a different Kalman filter for each value of the uncertain parameter. Figs. 3, 4 and 5 show these plots for $\mu_1 = 0.25, 0.5$ and 0.75 , respectively.

Clearly, the Kalman smoother behaves better than the robust smoother when $\delta_1 = 0$, as expected. However, as δ_1

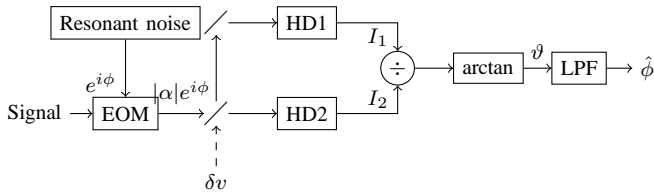


Fig. 2. Block diagram of the dual-homodyne scheme for deducing the SQL for the resonant noise.

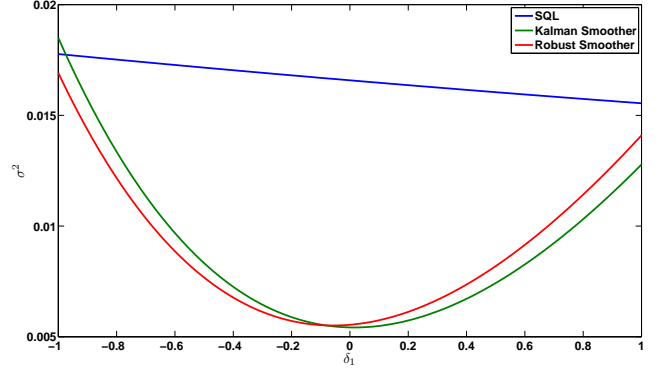


Fig. 3. Coherent State: Comparison of the smoothers for $\mu_1 = 0.25$ and $\mu_2 = 0$.

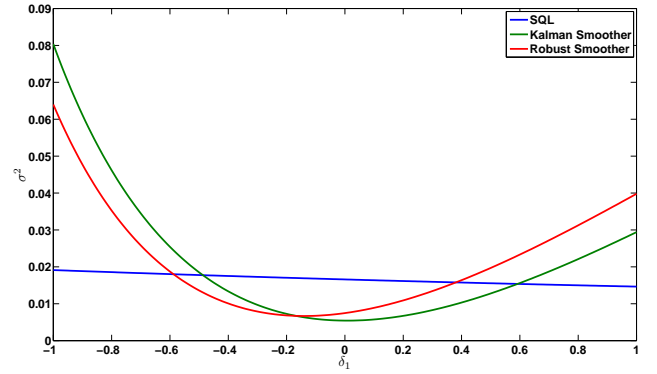


Fig. 4. Coherent State: Comparison of the smoothers for $\mu_1 = 0.5$ and $\mu_2 = 0$.

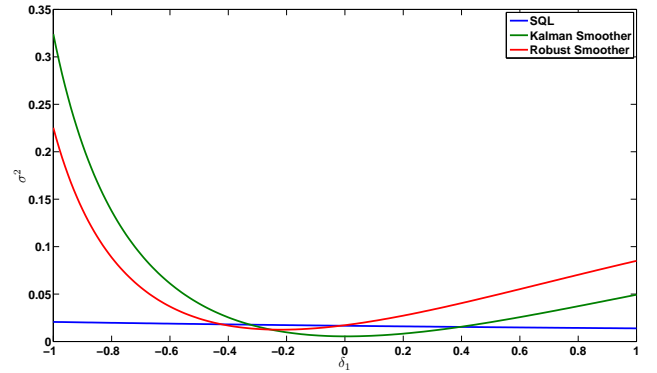


Fig. 5. Coherent State: Comparison of the smoothers for $\mu_1 = 0.75$ and $\mu_2 = 0$.

approaches -1 , the performance of the robust smoother is superior to that of the Kalman smoother for all levels of μ_1 . Also for $\mu_1 = 0.25$, the robust smoother is better than the SQL throughout the uncertainty window, while the Kalman smoother is not.

Similarly, the estimation mean-square errors may be calculated, and plots created, for the robust smoother and the

Kalman smoother as a function of the uncertain parameter δ_2 with $\delta_1 = 0$. Here, we choose different values for μ_2 and set $\mu_1 = 0$. Figs. 6 and 7 show these plots for $\mu_2 = 0.2$ and 0.5 , respectively. In this case, the robust and Kalman smoothers behave almost identically for all levels of μ_2 .

VI. SQUEEZED STATE CASE

We now consider a phase-squeezed beam as in Ref. [17], whose phase is modulated with the resonant noise process. The beam is then measured by homodyne detection using a local oscillator, the phase of which is adjusted according to the filtered estimate $\phi_f(t)$.

The normalized homodyne output current $I(t)$ is given by

$$I(t)dt \simeq 2|\alpha|[\phi(t) - \phi_f(t)]dt + \sqrt{\bar{R}_{sq}}dW(t), \quad (28)$$

$$\bar{R}_{sq} = \sigma_f^2 e^{2r_p} + (1 - \sigma_f^2)e^{-2r_m}, \quad (29)$$

where $|\alpha|$ is the amplitude of the input phase-squeezed beam, and $W(t)$ is a Wiener process arising from squeezed vacuum fluctuations. The parameter \bar{R}_{sq} is determined by the degree of squeezing ($r_m \geq 0$) and anti-squeezing ($r_p \geq r_m$) and by $\sigma_f^2 = \langle [\phi(t) - \phi_f(t)]^2 \rangle$.

The measurement model is, thus, [32]:

$$\theta = \mathbf{H}\mathbf{x} + w, \quad (30)$$

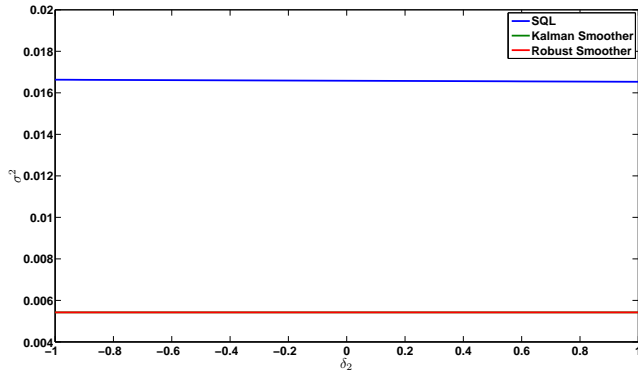


Fig. 6. Coherent State: Comparison of the smoothers for $\mu_2 = 0.2$ and $\mu_1 = 0$.

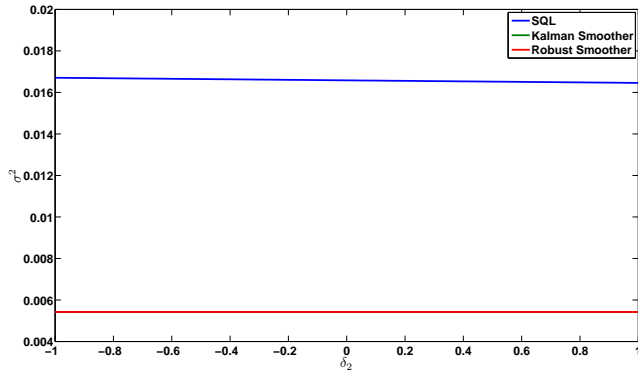


Fig. 7. Coherent State: Comparison of the smoothers for $\mu_2 = 0.5$ and $\mu_1 = 0$.

where $\mathbf{H} = \begin{bmatrix} 2|\alpha|/\sqrt{\bar{R}_{sq}} & 0 \end{bmatrix}$.

Eqs. (5) to (18) are then modified accordingly.

VII. SQUEEZED STATE: COMPARISON FOR THE ROBUST AND KALMAN SMOOTHERS

We use the Lyapunov method again, as described in section V-A, to compute the estimation mean-square errors for the robust smoother and the Kalman smoother, as a function of δ_1 with $\delta_2 = 0$. Here, we use the nominal values of the parameters, $r_m = 0.36$, $r_p = 0.59$ and chosen values for μ_1 with $\mu_2 = 0$. These values were used to generate plots of the errors versus δ_1 to compare the performance of the robust smoother and the Kalman smoother for the uncertain system in comparison to the CSL. Due to the implicit dependence of \bar{R}_{sq} and σ_f^2 , we compute the smoothed mean-square error in each case by running several iterations until σ_f^2 is obtained with an accuracy of 6 decimal places. The CSL value is obtained by designing, as described in section III, a different Kalman smoother for each value of the uncertain parameter in (12) (note $r_m, r_p = 0$ and $\bar{R}_{sq} = 1$ here), and is given by $\sigma^2 = \mathbf{P}_s(1, 1)$ from (10). Figs. 8, 9 and 10 show the plots for $\mu_1 = 0.3, 0.5$ and 0.6 , respectively. Note that as δ_1 approaches -1 , the performance of the robust smoother is better than that of the Kalman smoother for all levels of μ_1 .

We can similarly plot the mean-square errors of the two smoothers compared to the CSL as a function of δ_2 with $\delta_1 = 0, \mu_1 = 0$ for various values of μ_2 . Figs. 11 and 12 show these plots for $\mu_2 = 0.5$ and 0.8 , respectively. The Kalman and robust smoothers behave almost identically for all levels of μ_2 .

VIII. CONCLUSION

This work applies robust fixed-interval smoothing to homodyne phase estimation of coherent and squeezed states of light, when under the influence of a continuous-time resonant noise process. It presents a comparison of the robust smoother with the optimal smoother for the uncertain system in relation to the standard quantum limit for the coherent state case, and the coherent state limit for the squeezed state

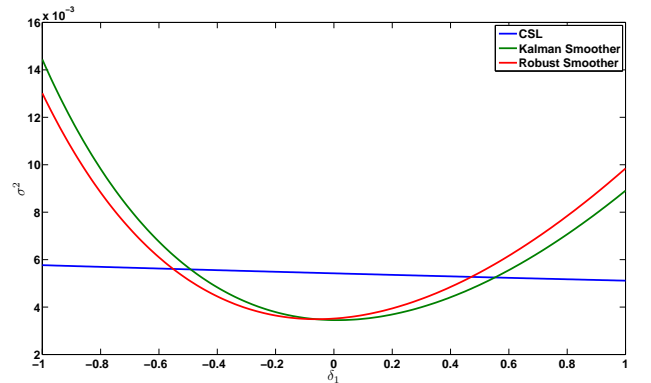


Fig. 8. Squeezed State: Comparison of the smoothers for $\mu_1 = 0.3$ and $\mu_2 = 0$.

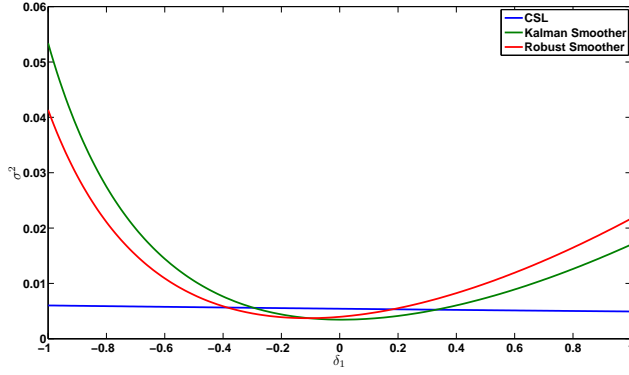


Fig. 9. Squeezed State: Comparison of the smoothers for $\mu_1 = 0.5$ and $\mu_2 = 0$.

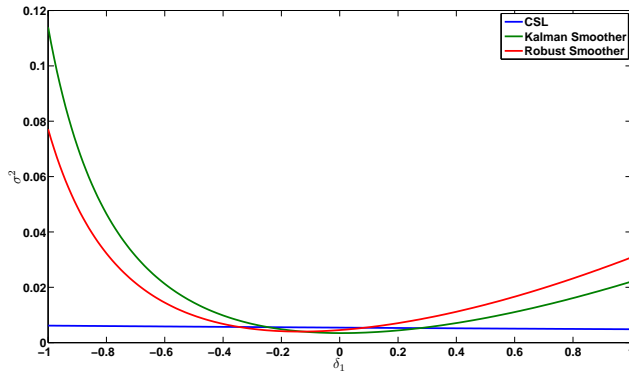


Fig. 10. Squeezed State: Comparison of the smoothers for $\mu_1 = 0.6$ and $\mu_2 = 0$.

case. These results may be demonstrated experimentally as further work.

REFERENCES

- [1] H. M. Wiseman and G. J. Milburn, *Quantum Measurement and Control*. Cambridge University Press, 2010.
- [2] V. Giovannetti, S. Lloyd, and L. Maccone, “Advances in quantum metrology,” *Nature Photonics*, vol. 5, p. 222, March 2011.

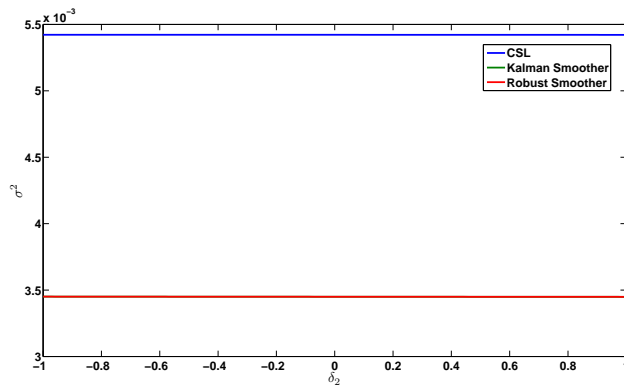


Fig. 11. Squeezed State: Comparison of the smoothers for $\mu_2 = 0.5$ and $\mu_1 = 0$.

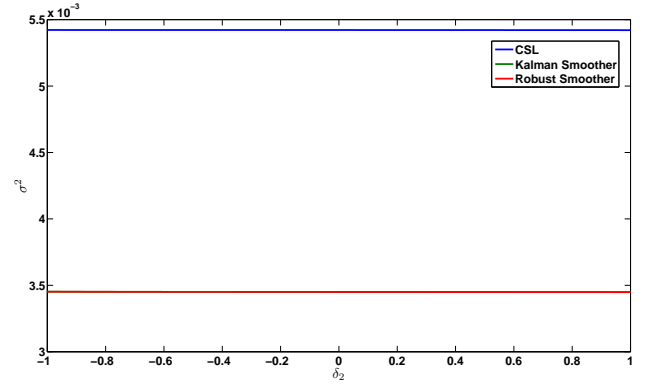


Fig. 12. Squeezed State: Comparison of the smoothers for $\mu_2 = 0.8$ and $\mu_1 = 0$.

- [3] M. Hofheinz, H. Wang, M. Ansmann, R. C. Bialczak, E. Lucero, M. Neeley, A. D. O’Connell, D. Sank, J. Wenner, J. M. Martinis, and A. N. Cleland, “Synthesizing arbitrary quantum states in a superconducting resonator,” *Nature (London)*, vol. 459, pp. 546–549, March 2009.
- [4] R. Slavik, F. Parmigiani, J. Kakande, C. Lundstrom, M. Sjodin, P. A. Andrekson, R. Weerasuriya, S. Sygletos, A. D. Ellis, L. Gruner-Nielsen, D. Jakobsen, S. Herstrom, R. Phelan, J. O’Gorman, A. Bogris, D. Syvridis, S. Dasgupta, P. Petropoulos, and D. J. Richardson, “All-optical phase and amplitude regenerator for next-generation telecommunications systems,” *Nature Photonics*, vol. 4, pp. 690–695, September 2010.
- [5] J. Chen, J. L. Habif, Z. Dutton, R. Lazarus, and S. Guha, “Optical codeword demodulation with error rates below the standard quantum limit using a conditional nulling receiver,” *Nature Photonics*, vol. 6, p. 374, May 2012.
- [6] K. Inoue, E. Waks, and Y. Yamamoto, “Differential phase shift quantum key distribution,” *Physical Review Letters*, vol. 89, p. 037902, June 2002.
- [7] V. Giovannetti, S. Lloyd, and L. Maccone, “Quantum-enhanced measurements: Beating the standard quantum limit,” *Science*, vol. 306, no. 5700, pp. 1330–1336, November 2004.
- [8] K. Goda, O. Miyakawa, E. E. Mikhailov, S. Saraf, R. Adhikari, K. McKenzie, R. Ward, S. Vass, A. J. Weinstein, and N. Mavalvala, “A quantum-enhanced prototype gravitational-wave detector,” *Nature Physics*, vol. 4, pp. 472–476, March 2008.
- [9] H. M. Wiseman, “Adaptive phase measurements of optical modes: Going beyond the marginal Q distribution,” *Physical Review Letters*, vol. 75, pp. 4587–4590, December 1995.
- [10] H. M. Wiseman and R. B. Killip, “Adaptive single-shot phase measurements: A semiclassical approach,” *Physical Review A*, vol. 56, pp. 944–957, July 1997.
- [11] H. M. Wiseman and R. B. Killip, “Adaptive single-shot phase measurements: The full quantum theory,” *Physical Review A*, vol. 57, pp. 2169–2185, March 1998.
- [12] M. A. Armen, J. K. Au, J. K. Stockton, A. C. Doherty, and H. Mabuchi, “Adaptive homodyne measurement of optical phase,” *Physical Review Letters*, vol. 89, p. 133602, September 2002.
- [13] D. W. Berry and H. M. Wiseman, “Phase measurements at the theoretical limit,” *Physical Review A*, vol. 63, p. 013813, December 2000.
- [14] D. W. Berry and H. M. Wiseman, “Adaptive quantum measurements of a continuously varying phase,” *Physical Review A*, vol. 65, p. 043803, March 2002.
- [15] M. Tsang, J. H. Shapiro, and S. Lloyd, “Quantum theory of optical temporal phase and instantaneous frequency. ii. continuous-time limit and state-variable approach to phase-locked loop design,” *Physical Review A*, vol. 79, p. 053843, May 2009.
- [16] T. A. Wheatley, D. W. Berry, H. Yonezawa, D. Nakane, H. Arao, D. T. Pope, T. C. Ralph, H. M. Wiseman, A. Furusawa, and E. H. Huntington, “Adaptive optical phase estimation using time-symmetric quantum smoothing,” *Physical Review Letters*, vol. 104, p. 093601, March 2010.

- [17] H. Yonezawa, D. Nakane, T. A. Wheatley, K. Iwasawa, S. Takeda, H. Arao, K. Ohki, K. Tsumura, D. W. Berry, T. C. Ralph, H. M. Wiseman, E. H. Huntington, and A. Furusawa, "Quantum-enhanced optical-phase tracking," *Science*, vol. 337, no. 6101, p. 1514, September 2012.
- [18] M. Tsang, "Time-symmetric quantum theory of smoothing," *Physical Review Letters*, vol. 102, p. 250403, June 2009.
- [19] L. Ljung and T. Kailath, "A unified approach to smoothing formulas," *Automatica*, vol. 12, no. 2, pp. 147–157, March 1976.
- [20] J. S. Meditch, "A survey of data smoothing for linear and nonlinear dynamic systems," *Automatica*, vol. 9, no. 2, pp. 151–162, March 1973.
- [21] J. E. Wall Jr., A. S. Willsky, and N. R. Sandell Jr., "On the fixed-interval smoothing problem," *Stochastics*, vol. 5, no. 1-2, pp. 1–41, 1981.
- [22] D. Q. Mayne, "A solution of the smoothing problem for linear dynamic systems," *Automatica*, vol. 4, no. 2, pp. 73–92, December 1966.
- [23] D. C. Fraser, "A new technique for the optimal smoothing of data," Sc.D. Dissertation, Massachusetts Institute of Technology, Cambridge, MA, January 1967.
- [24] R. K. Mehra, "Studies in smoothing and in conjugate gradient methods applied to optimal control problems," Ph.D. Dissertation, Harvard University, Cambridge, MA, May 1967.
- [25] D. C. Fraser and J. E. Potter, "The optimum linear smoother as a combination of two optimum linear filters," *IEEE Transactions on Automatic Control*, vol. 14, no. 4, pp. 387–390, August 1969.
- [26] H. E. Rauch, F. Tung, and C. T. Striebel, "Maximum likelihood estimates of linear dynamic systems," *AIAA Journal*, vol. 3, no. 8, pp. 1445–1450, August 1965.
- [27] F. L. Lewis, L. Xie, and D. Popa, *Optimal and Robust Estimation - With an Introduction to Stochastic Control Theory*, 2nd ed. CRC Press, Taylor & Francis Group, 2008.
- [28] S. Roy, I. R. Petersen, and E. H. Huntington, "Robust filtering for adaptive homodyne estimation of continuously varying optical phase," *Proceedings of the 2012 Australian Control Conference*, pp. 454–458, November 2012.
- [29] I. R. Petersen and D. C. McFarlane, "Optimal guaranteed cost control and filtering for uncertain linear systems," *IEEE Transactions on Automatic Control*, vol. 39, no. 9, pp. 1971–1977, September 1994.
- [30] S. O. R. Moheimani, A. V. Savkin, and I. R. Petersen, "Robust filtering, prediction, smoothing, and observability of uncertain systems," *IEEE Trans. on Circuits and Systems I - Fundamental Theory and Appl.*, vol. 45, no. 4, p. 446, April 1998.
- [31] S. Roy, I. R. Petersen, and E. H. Huntington, "Adaptive continuous homodyne phase estimation using robust fixed-interval smoothing," *To appear in the Proceedings of the American Control Conference, 2013*.
- [32] S. Roy, I. R. Petersen, and E. H. Huntington, "Robust phase estimation of squeezed state," *Proceedings of the CLEO:QELS 2013, submitted*.
- [33] S. Roy, I. R. Petersen, and E. H. Huntington, "Robust estimation of optical phase varying as a continuous resonant process," *Proceedings of the Multiconference on Systems and Control 2013, submitted*.
- [34] R. G. Brown, *Introduction to Random Signal Analysis and Kalman Filtering*. John Wiley & Sons, 1983.